

2

AD-A275 159



NAVAL POSTGRADUATE SCHOOL MONTEREY, CALIFORNIA



DTIC
JAN 1 1994

THESIS

FEEDBACK CONTROL OF A THREE-LINK
PLANAR UNDER-ACTUATED MANIPULATOR
USING A "SURGE" VELOCITY

by

Pernell A. Jordan

September, 1993

Thesis Advisor:

Ranjan Mukherjee

Approved for public release; distribution is unlimited

94-02741



1478

94 1 26 1 5

REPORT DOCUMENTATION PAGE

Form Approved OMB No. 0704

Public reporting burden for this collection of information is estimated to average 1 hour per response, including the time for reviewing instruction, searching existing data sources, gathering and maintaining the data needed, and completing and reviewing the collection of information. Send comments regarding this burden estimate or any other aspect of this collection of information, including suggestions for reducing this burden, to Washington headquarters Services, Directorate for Information Operations and Reports, 1215 Jefferson Davis Highway, Suite 1204, Arlington, VA 22202-4302, and to the Office of Management and Budget, Paperwork Reduction Project (0704-0188) Washington DC 20503.

1. AGENCY USE ONLY		2. REPORT DATE 23 September 1993	3. REPORT TYPE AND DATES COVERED Master's Thesis	
4. TITLE AND SUBTITLE FEEDBACK CONTROL OF A THREE-LINK PLANAR UNDER-ACTUATED MANIPULATOR USING A "SURGE" VELOCITY			5. FUNDING NUMBERS	
6. AUTHOR(S) Pernell Arthur Jordan				
7. PERFORMING ORGANIZATION NAME(S) AND ADDRESS(ES) Naval Postgraduate School Monterey, CA 93943-5000			8. PERFORMING ORGANIZATION REPORT NUMBER	
9. SPONSORING/MONITORING AGENCY NAME(S) AND ADDRESS(ES) Naval Surface Warfare Center			10. SPONSORING/MONITORING AGENCY REPORT NUMBER Code 2814	
11. SUPPLEMENTARY NOTES The views expressed in this thesis are those of the author and do not reflect the official policy or position of the Department of Defense or the U.S. Government.				
12a. DISTRIBUTION/AVAILABILITY STATEMENT Approved for public release; distribution is un'limited.			12b. DISTRIBUTION CODE A	
13. ABSTRACT An under-actuated robot manipulator is one that has fewer number of joint actuators than the number of degrees of freedom of the manipulator. Such manipulators are studied with the objective of developing "smarter" mechanical systems; ones that can provide low-cost automation, and enable design simplification. While in space these manipulators can afford to have any kind of mechanical structure, on earth they need to be strictly planar to be feasible. In this paper, we develop a control scheme for a three link planar robot manipulator with two actuators such that it can reach any joint configuration from any other. We assume that the first joint of the robot is passive, and is provided with a brake and a rotary dashpot. We show that our control is robust to the variations in certain parameters and unmodelled dynamics like stiction.				
14. SUBJECT TERMS LYAPUNOV FUNCTION, KINEMATIC APPROACH, DYNAMIC APPROACH, "SURGE" VELOCITY, UNDER-ACTUATED MANIPULATOR			15. NUMBER OF PAGES 47	
			16. PRICE CODE	
17. SECURITY CLASSIFICATION OF REPORT Unclassified	18. SECURITY CLASSIFICATION OF THIS PAGE Unclassified	19. SECURITY CLASSIFICATION OF ABSTRACT Unclassified	20. LIMITATION OF ABSTRACT UL	

Approved for public release; distribution is unlimited.

Feedback Control of a Three-Link
Planar Under-Actuated Manipulator
Using a "Surge" Velocity

by

Pernell A. Jordan
Lieutenant, United States Navy
B.S., Norfolk State University 1987

Submitted in partial fulfillment of the
requirements for the degree of

MASTER OF SCIENCE IN MECHANICAL ENGINEERING

from the

NAVAL POSTGRADUATE SCHOOL

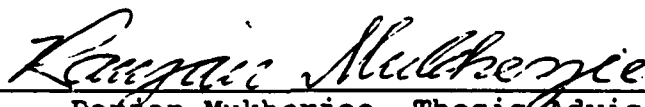
September 1993

Author:



Pernell A. Jordan

Approved by:



Ranjan Mukherjee, Thesis Advisor



Matthew D. Kelleher, Chairman
Department of Mechanical Engineering

ABSTRACT

An under-actuated robot manipulator is one that has fewer number of joint actuators than the number of degrees of freedom of the manipulator. Such manipulators are studied with the objective of developing "smarter" mechanical systems; ones that can provide low-cost automation, and enable design simplification. While in space these manipulators can afford to have any kind of mechanical structure, on earth they need to be strictly planar to be feasible. In this paper, we develop a control scheme for a three link planar robot manipulator with two actuators such that it can reach any joint configuration from any other. We assume that the first joint of the robot is passive, and is provided with a brake and a rotary dashpot. We show that our control is robust to the variations in certain parameters and unmodelled dynamics like stiction.

DTIC QUALITY INSPECTED 6

Accession For	
NTIS CRA&I	<input checked="" type="checkbox"/>
DTIC TAB	<input type="checkbox"/>
Unannounced	<input type="checkbox"/>
Justification	
By	
Distribution/	
Availability Codes	
Dist	Avail and/or Special
A-1	

TABLE OF CONTENTS

I INTRODUCTION 1

**II DYNAMICS OF A PLANAR THREE-LINK UNDER-ACTUATED
MANIPULATOR 4**

**III CONTROL OF AN UNDER-ACTUATED MANIPULATOR IN JOINT
SPACE 10**

**A. DYNAMICS OF A PLANAR MANIPULATOR WHOSE FIRST LINK
IS NOT ACTUATED 10**

B. CONTROLLING ALL THE JOINTS OF THE MANIPULATOR . 12

**C. PARAMETRIC UNCERTAINTIES AND UNMODELLED
DYNAMICS 16**

IV RESULTS AND DISCUSSION 21

**A. CONTROLLING OF JOINTS IN THE ABSENCE OF
UNCERTAINTIES 21**

B. CONTROLLING OF JOINTS WITH UNCERTAINTIES . . . 24

1. Variation of damping without stiction . . . 24

2. Variation of damping with stiction 29

a. Variation of damping given by Eq.(4.3) . 29

b. Variation of damping given by Eq.(4.4) . 32

V	CONCLUSIONS AND RECOMMENDATIONS	35
	LIST OF REFERENCES	37
	INITIAL DISTRIBUTION LIST	38

LIST OF FIGURES

<p>Figure 1: A three link planar under-actuated manipulator is shown whose first joint is passive. The passive joint has a brake and a rotary dashpot.</p>	5
<p>Figure 2: Evolution of joints for case one</p>	23
<p>Figure 3: Evolution of joints for case two</p>	23
<p>Figure 4a: Damping of the form described by Eq.(4.3) .</p>	25
<p>Figure 4b: Damping of the form described by Eq.(4.4) .</p>	26
<p>Figure 5a: Evolution of joints for case one under influence of damping given by Eq.(4.3) . . .</p>	27
<p>Figure 5b: Evolution of θ_{2d} for case one under influence of damping given by Eq.(4.3) . . .</p>	27
<p>Figure 6a: Evolution of joints for case one under influence of damping given by Eq.(4.4) . . .</p>	28
<p>Figure 6b: Evolution of θ_{2d} for case one under influence of damping given by Eq.(4.4) . . .</p>	28
<p>Figure 7a: Evolution of joints for case one under influence of damping given by Eq.(4.3) and a stiction value of 0.001.</p>	30
<p>Figure 7b: Evolution of θ_{2d} for case one under influence of damping given by Eq.(4.3) and a stiction value of 0.001</p>	30
<p>Figure 8a: Evolution of joints for case two under</p>	

	influence of damping given by Eq.(4.3) and a stiction value of 0.001	31
Figure 8b:	Evolution of θ_{2d} for case two under influence of damping given by Eq.(4.3) and a stiction value of 0.001	31
Figure 9a:	Evolution of joints for case one under influence of damping given by Eq.(4.4) and a stiction value of 0.005	33
Figure 9b:	Evolution of θ_{2d} for case one under influence of damping given by Eq.(4.4) and a stiction value of 0.005	33
Figure 10a:	Evolution of joints for case two under influence of damping given by Eq.(4.4) and a stiction value of 0.005	34
Figure 10b:	Evolution of θ_{2d} for case two under influence of damping given by Eq.(4.4) and a stiction value of 0.005	34

I INTRODUCTION

Robot manipulators with passive joints have been studied by a few researchers for terrestrial and space applications [1], [2], [3], [4]. In space, such manipulators can have any kinematic configuration because of the absence of gravity but on earth the concept of under-actuation can only be promoted among planar kinematic configurations. The purpose of this research is to look into the possibility of successfully using under-actuated manipulators on earth. Arai and Tachi [1] surmised that it would be difficult to control both the passive and active joints simultaneously to reach the desired position precisely while the passive joints are free. They maintained that control is easier using a brakes-on period while the actuated links are providing momentum to the unactuated link followed by a brakes-off period which will allow the unactuated joint to converge to its final position. The mechanism would then apply brakes and allow the actuated joints to converge to its final position. Simulations were demonstrated using a two degree of freedom manipulator. We will consider the point to point control of a three-link planar manipulator with two actuators and a passive first joint. We will provide a surge velocity in order to allow the unactuated joint to converge to its desired position.

Robot manipulators with passive joints are unconventional but there is a great potential for using such systems. On earth, under-actuated manipulators will enable design simplification and provide low-cost automation. The most significant part of the design of a robot manipulator lies in the selection of its actuators, the design task will be simplified to a great extent. Also, the actuators along with the drive accounts for a significant part of the cost of a robotic system. With fewer actuators, an under-actuated manipulator will be cheaper than a conventional manipulator. However, the power consumption of an under-actuated manipulator may not be less than that of a completely actuated system. The concept of under-actuation can also be applied to a completely actuated system with actuator failures. This is particularly useful for space applications where repair or replacement may not be an easy task.

Jain and Rodriguez [2] developed the kinematics and the dynamics of under-actuated manipulators. They used the techniques from the spatial operator algebra to develop expression for the generalized Jacobian, the mass matrix and an efficient inverse dynamics algorithm. The spatial operator is a robot modeling and analysis framework which is used to provide a compact description of the robot model and to derive efficient recursive algorithms for robotics computations. This algorithm is a hybrid combinations of well known inverse

and forward dynamics algorithms for fully-actuated manipulators.

In this paper, we consider the control problem of a three-link planar under-actuated manipulator using the Lagrangian approach to develop the equations of motion. We assume the passive joint to be equipped with a brake that will be used for tasks like force control, and for the switching of control inputs. Additionally, the passive joint will have a rotary dashpot for greater control, and a position sensor feedback. Clearly, we are considering a completely different class of mechanical systems where some of the actuators are replaced by viscous dampers. These systems will be cheaper and will be easier to design but will not necessarily provide solutions to systems with actuator failures. The simulations of the three-link planar under-actuated manipulator will be studied in the following manner:

1. The damping at the unactuated joint is constant and there are no parametric uncertainties or unmodelled dynamics.
2. The damping at the unactuated joint is not constant and varies randomly with time.
3. The damping at the unactuated joint varies randomly in time and there is also stiction at the first joint.

II DYNAMICS OF A PLANAR THREE-LINK UNDER-ACTUATED MANIPULATOR

The equations of motion for the manipulator will be derived considering the way in which torque cause motion. We adopt the Lagrangian approach to solve this problem. The Lagrangian dynamics approach is an energy based approach to dynamics. In this section we develop the equation of motion of the three link under actuated manipulator. The Lagrangian is defined as

$$L=T-V \quad (2.1)$$

where, T and V are the kinetic energy and potential energy of the system. The kinetic energy is a function of both the joint position and velocities. The potential energy for the system is equal to zero due to the absence of gravity in space. While considering Figure 1, we compute the position vectors as

$$r_1 = \frac{l_1}{2} \cos \theta_2 i + \frac{l_1}{2} \sin \theta_1 j$$

$$r_2 = [l_1 \cos \theta_1 + \frac{l_2}{2} \cos (\theta_1 + \theta_2)] i + [l_1 \sin \theta_1 + \frac{l_2}{2} \sin (\theta_1 + \theta_2)] j$$

$$r_3 = [l_1 \cos \theta_1 + l_2 \cos (\theta_1 + \theta_2) + \frac{l_3}{2} \cos (\theta_1 + \theta_2 + \theta_3)] i$$

$$+ [l_1 \sin \theta_1 + l_2 \sin (\theta_1 + \theta_2) + \frac{l_3}{2} \sin (\theta_1 + \theta_2 + \theta_3)] j$$

(2.2)

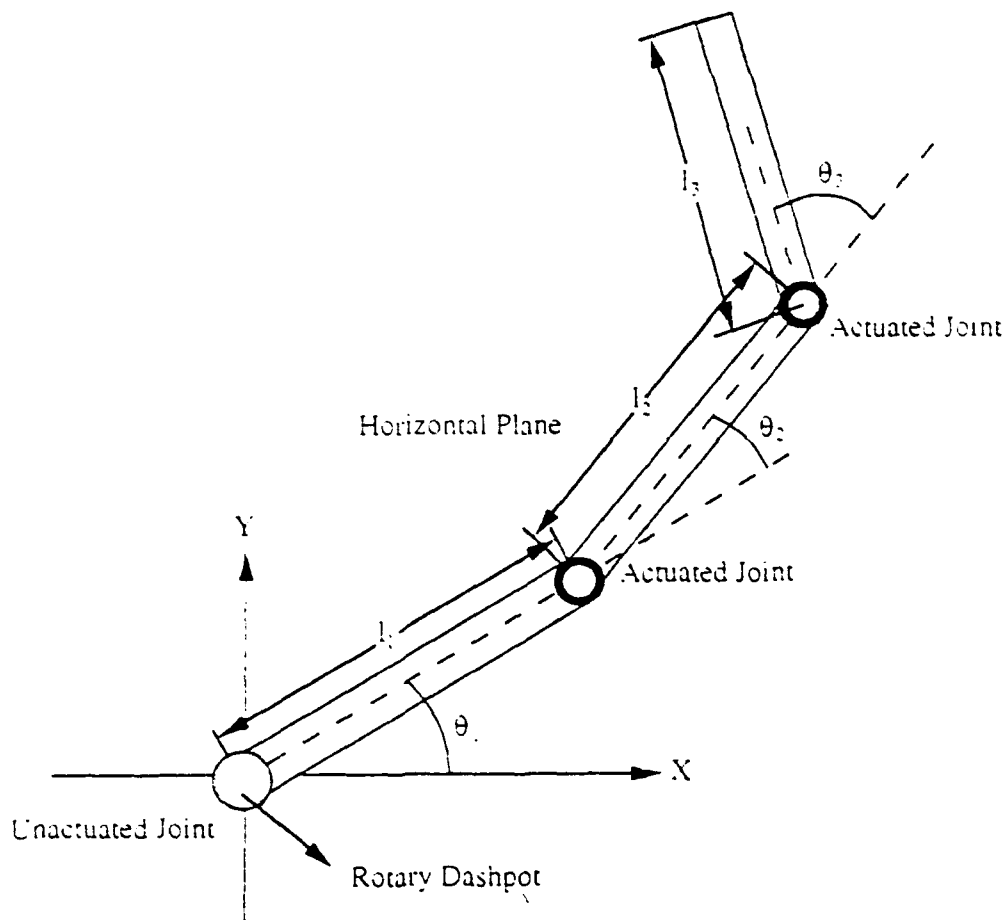


Figure 1: A three link planar under-actuated manipulator is shown whose first joint is passive. The passive joint has a brake and a rotary dashpot.

From Eq. (2.2) we compute the linear velocities of each link as

$$\begin{aligned} \dot{r}_1 &= -\frac{l_1}{2} \sin \theta_1 \dot{\theta}_1 i + \frac{l_1}{2} \cos \theta_1 \dot{\theta}_1 j \\ \dot{r}_2 &= [-l_1 \sin \theta_1 \dot{\theta}_1 - \frac{l_2}{2} \sin (\theta_1 + \theta_2) (\dot{\theta}_1 + \dot{\theta}_2)] i \\ &\quad + [l_1 \cos \theta_1 \dot{\theta}_1 + \frac{l_2}{2} \cos (\theta_1 + \theta_2) (\dot{\theta}_1 + \dot{\theta}_2)] j \\ \dot{r}_3 &= [-l_1 \sin \theta_1 \dot{\theta}_1 - l_2 \sin (\theta_1 + \theta_2) (\dot{\theta}_1 + \dot{\theta}_2) + \frac{l_3}{2} \sin (\theta_1 + \theta_2 + \theta_3) (\dot{\theta}_1 + \dot{\theta}_2 + \dot{\theta}_3)] i \\ &\quad + [l_1 \cos \theta_1 \dot{\theta}_1 + l_2 \cos (\theta_1 + \theta_2) (\dot{\theta}_1 + \dot{\theta}_2) + \frac{l_3}{2} \cos (\theta_1 + \theta_2 + \theta_3) (\dot{\theta}_1 + \dot{\theta}_2 + \dot{\theta}_3)] j \end{aligned} \quad (2.3)$$

from which we can compute the total kinetic energy. The total kinetic energy is equal to

$$K.E. = \frac{1}{2} m_1 \dot{r}_1^2 + \frac{1}{2} m_2 \dot{r}_2^2 + \frac{1}{2} m_3 \dot{r}_3^2 + \frac{1}{2} I_1 \dot{\theta}_1^2 + I_2 (\dot{\theta}_1 + \dot{\theta}_2)^2 + \frac{1}{2} I_3 (\dot{\theta}_1 + \dot{\theta}_2 + \dot{\theta}_3)^2 \quad (2.4)$$

where I is defined as the inertia. The expanded version of the kinetic energy is

$$\begin{aligned} K.E. &= \frac{1}{2} m_1 \left(\frac{l_1^2}{4} \dot{\theta}_1^2 \right) + \frac{1}{2} m_2 \left[l_1^2 \dot{\theta}_1^2 + \frac{l_2^2}{4} (\dot{\theta}_1 + \dot{\theta}_2)^2 + l_1 l_2 \dot{\theta}_1 (\dot{\theta}_1 + \dot{\theta}_2) \cos \theta_2 \right] \\ &\quad + \frac{1}{2} m_3 \left[l_1^2 \dot{\theta}_1^2 + l_2^2 (\dot{\theta}_1 + \dot{\theta}_2)^2 + \frac{l_3^2}{4} (\dot{\theta}_1 + \dot{\theta}_2 + \dot{\theta}_3)^2 + 2 l_1 l_2 \dot{\theta}_1 (\dot{\theta}_1 + \dot{\theta}_2) \cos \theta_2 \right] \end{aligned}$$

$$\begin{aligned}
& +l_1 l_3 \theta_1 (\theta_1 + \theta_2 + \theta_3) \cos (\theta_2 + \theta_3) + l_2 l_3 (\theta_1 + \theta_2) (\theta_1 + \theta_2 + \theta_3) \cos \theta_3 \\
& + \frac{1}{2} I_1 \theta_1^2 + \frac{1}{2} I_2 (\theta_1 + \theta_2)^2 + \frac{1}{2} I_3 (\theta_1 + \theta_2 + \theta_3)^2
\end{aligned}
\tag{2.5}$$

The Kinetic energy in matrix form is

$$K.E. = \frac{1}{2} (\theta_1 \theta_2 \theta_3) \begin{pmatrix} A_{11} & A_{12} & A_{13} \\ A_{21} & A_{22} & A_{23} \\ A_{31} & A_{32} & A_{33} \end{pmatrix} \begin{pmatrix} \theta_1 \\ \theta_2 \\ \theta_3 \end{pmatrix}
\tag{2.6}$$

where,

$$A_{11} = (m_1 \frac{l_1^2}{4} + m_2 l_1^2 + m_2 \frac{l_2^2}{4} + m_2 l_1 l_2 \cos \theta_2 + m_3 l_2^2 + m_3 \frac{l_3^2}{4} + 2m_3 l_1 l_2 \cos \theta_2$$

$$+ m_3 l_1 l_3 \cos (\theta_2 + \theta_3) + m_3 l_2 l_3 \cos \theta_3 + I_1 + I_2 + I_3$$

$$A_{12} = m_2 \frac{l_2^2}{4} + \frac{1}{2} m_2 l_1 l_2 \cos \theta_2 + m_3 l_2^2 + m_3 \frac{l_3^2}{4} + m_3 l_1 l_2 \cos \theta_2$$

$$+ \frac{1}{2} m_3 l_1 l_3 \cos (\theta_2 + \theta_3) + m_3 l_2 l_3 \cos \theta_3 + I_2 + I_3$$

$$A_{13} = m_3 \frac{l_3^2}{4} + \frac{1}{2} m_3 l_1 l_3 \cos (\theta_2 + \theta_3) + \frac{1}{2} m_3 l_2 l_3 \cos \theta_3 + I_3$$

$$A_{21} = A_{12}$$

$$A_{22} = m_2 \frac{l_2^2}{4} + M_3 l_2^2 + m_3 \frac{l_3^2}{4} + m_3 l_2 l_3 \cos \theta_3 + I_2 + I_3$$

$$A_{23} = m_3 \frac{l_3^2}{4} + \frac{1}{2} m_3 l_2 l_3 \cos \theta_3 + I_3$$

$$A_{33} = m_3 \frac{l_3^2}{4} + I_3$$

$$A_{31} = A_{13}$$

$$A_{32} = A_{23}$$

(2.7)

From Eq.(2.6), the Lagrangian is computed as

$$L = 0.5 (A_{11} \dot{\theta}_1^2 + 2A_{12} \dot{\theta}_1 \dot{\theta}_2 + 2A_{13} \dot{\theta}_1 \dot{\theta}_3 + A_{22} \dot{\theta}_2^2 + 2A_{23} \dot{\theta}_2 \dot{\theta}_3 + A_{33} \dot{\theta}_3^2)$$

(2.8)

The equation of motion for our three degree of freedom manipulator can be written as

$$\frac{d}{dt} (\partial L / \partial \dot{\theta}_i) - \partial L / \partial \theta_i = \tau_i, (i=1-3)$$

(2.9)

where we assume the first joint of our manipulator of be passive. The second term of Eq.(2.9), $\partial L / \partial \theta_1$, equals zero because L is not a function of θ_1 . The third term of Eq.(2.9), τ_1 , is also equal to zero since no torque is applied

applied at the first joint (in the case where there are no external generalized forces corresponding to θ_1).

III CONTROL OF AN UNDER-ACTUATED MANIPULATOR IN JOINT SPACE

A. DYNAMICS OF A PLANAR MANIPULATOR WHOSE FIRST LINK IS NOT ACTUATED

In this section we consider the dynamics of a three-link planar under-actuated robot manipulator with revolute joints. The manipulator is assumed to be planar primarily because we would like to investigate the possibility of using such manipulators on earth. In the past under-actuated space manipulators have been considered [3]. We consider the manipulator to have three links because a minimum of three degrees of freedom is required to perform tasks with dexterity. Our current research is aimed at studying the feasibility of a three-link manipulator where the first joint of the manipulator does not have an actuator. The passive joint is however provided with a brake and a rotary dashpot. The brake is essential if the manipulator has to perform tasks like force control and for switching of control inputs. The dashpot provides us with improved control over the system. The passive joint is also equipped with a position sensor.

The joints of the robotic system are designated as θ_1 , θ_2 , and θ_3 where, θ_1 is the only unactuated joint. The choice of the location of the unactuated joint is motivated by two factors: (a) The first motor of the robot is design to be the

most powerful actuator and its elimination will save the maximum cost. (b) The first joint of the robot is a cyclic coordinate, that allows us to partially integrate the corresponding differential equation when there are no generalized forces acting at the first joint. If the Lagrangian of the system is L , the equation of motion for the first joint can be written as

$$\frac{d}{dt} (\partial L) / (\partial \dot{\theta}_1) = 0 \tag{3.1}$$

When there are no external generalized forces acting at the first joint, Equation (3.1) can be simplified to the form

$$A_{11}\ddot{\theta}_1 + A_{12}\ddot{\theta}_2 + A_{13}\ddot{\theta}_3 = k \tag{3.2}$$

where k is a constant that depends upon the initial conditions. A_{11} , A_{12} , and A_{13} elements of the mass matrix of the system were found from Eq.(2.7).

We now include passive damping at the unactuated joint of the robot using a rotary dashpot. If the damping constant of the rotary dashpot is assumed to be C , then Eq(3.2) would be modified to the form

$$A_{11}\ddot{\theta}_1 + A_{12}\ddot{\theta}_2 + A_{13}\ddot{\theta}_3 + C\dot{\theta}_1 = K \tag{3.3}$$

The above equation acts as a scleronomic constraint on the motion of the system. From this equation it is clear that if

the constant K is zero, then the first joint behaves as a first order system whenever the actuated joints θ_2 and θ_3 have zero velocity. This means that if the actuated joints stop, the first joint exponentially converges to the configuration $\theta_1=0$ with a convergence rate of C/A_{11} . We note here that A_{11} is a constant whenever the actuated joints are held fixed. If the initial conditions of the system are such that K is equal to $C\theta_{1d}$ then the first joint will exponentially converge to the configuration θ_{1d} after the actuated joints have stopped moving.

B. CONTROLLING ALL THE JOINTS OF THE MANIPULATOR

In this section we develop a control law that will enable us to converge all the joints of the manipulator from an initial configuration to its desired configuration. In this section we assume that there are no parametric uncertainties and the dynamics of the system given by Eq.(3.3) is an accurate model.

From our discussion in the previous section, we have seen that if the constant K is chosen appropriately, the first joint can be made to exponentially converge to any desired configuration by simply setting the actuated joints to zero velocity. Therefore, if all the joints of the manipulator need to be converged, we can converge the actuated joints first and then hold them fixed at their desired configuration. The unactuated joint will then converge to its desired

configuration θ_{1d} . This raises two questions: (a) How can we choose K to converge the actuated joint to its desired configuration? (b) What will be the time constant of the exponential convergence of the first joint once the actuated joints stop moving?

We answer the second question first. The term A_{11} represents the total inertia of the planar manipulator about the first joint. The magnitude of the damping constant C will be small as compared to the magnitude of A_{11} for all practical purposes. Therefore, the time constant for the exponential convergence of the first joint, given by A_{11}/C , will be quite large. Due to the large value of the time constant, the approach discussed above for the convergence of all the joints of the manipulator becomes impractical.

Before we modify our approach for the convergence of all the joints of the manipulator, we answer the question pertaining to the correct choice of the constant K . Let us suppose that the initial configuration of the unactuated joint is θ_{1i} , and let us assume that all the joints of the manipulator have zero velocity at the initial point of time. Then from Eq. (3.4) the value of the constant K is going to be $C\theta_{1i}$. For setting up the initial conditions such that the constant K is equal to $C\theta_{1d}$, we can adopt the following approach. We apply the brake at the unactuated joint to keep its configuration fixed at θ_{1i} . We also use the actuator at the third joint to keep the configuration of the third joint

fixed. We can actuate the second joint of the manipulator to achieve a velocity of $\dot{\theta}_2$ such that

$$A_{12}\dot{\theta}_2 = c(\theta_1 d - \theta_{1d}) \quad (3.4)$$

This velocity will not be a constant velocity because A_{12} is a function of θ_2 itself. Once Eq.(3.5) is satisfied, we will free the unactuated joint. This will now set the value of the constant in Eq.(3.3) as $K = C\theta_{1d}$, and we will have the dynamical equation

$$A_{11}\dot{\theta}_1 + A_{12}\dot{\theta}_2 + A_{13}\dot{\theta}_3 + c(\theta_1 - \theta_{1d}) = 0 \quad (3.5)$$

The initial velocity of one of the actuated joints that provide us with the necessary initial condition will be termed as the "surge" velocity.

To converge all the joints of the manipulator to their desired configuration with a satisfactory rate of convergence, we define the Lyapunov function V_1 in the following way

$$V_1 = 0.5 (\beta_1 \Delta\theta_1^2 + \beta_2 \Delta\theta_2^2 + \beta_3 \Delta\theta_3^2) + \Delta\theta_i \Delta(\theta_{id} - \theta_i), i=1, 2, 3 \quad (3.6)$$

where, $\beta_1, \beta_2, \beta_3$ are positive constants, and θ_{id} and θ_i are the desired and the current configurations of the i -th joint of the manipulator. The derivative of the Lyapunov function can be computed using Eq.(3.3) as

$$(3.7)$$

$$\dot{V}_1 = -\dot{\theta}_2 \left(\beta_2 \Delta \theta_2 - \beta_1 \frac{A_{12}}{A_{11}} \Delta \theta_1 \right) - \dot{\theta}_3 \left(\beta_3 \Delta \theta_3 - \beta_1 \frac{A_{13}}{A_{11}} \Delta \theta_1 \right) - \beta_1 \frac{C}{A_{11}} \Delta \theta_1^2$$

where A_{11} is not equal to zero because the mass matrix is positive definite. In the above equation, if we choose the joint velocities of the actuated joints as our inputs, then the choice

$$\dot{\theta}_2 = \left(\beta_2 \Delta \theta_2 - \beta_1 \frac{A_{12}}{A_{11}} \Delta \theta_1 \right), \dot{\theta}_3 = \left(\beta_3 \Delta \theta_3 - \beta_1 \frac{A_{13}}{A_{11}} \Delta \theta_1 \right) \quad (3.8)$$

can be shown to result in the globally asymptotically stable control that will drive the system to its desired configuration. The joint torques τ_2 and τ_3 that produce the desired joint velocities $\dot{\theta}_2$ and $\dot{\theta}_3$ given in Eq.(3.8) can be obtained by simply performing the inverse dynamics computation, or better yet by redefining the Lyapunov function in the following way

$$V_2 = V_1 + H \quad (3.9)$$

where H is the Hamiltonian of the system and is equal to the total kinetic energy of the under-actuated manipulator system. By knowing that

$$\dot{H} = -c\dot{\theta}_1^2 + \dot{\theta}_2 \tau_2 + \dot{\theta}_3 \tau_3$$

the derivative of V_2 can be shown to be negative definite when the control inputs τ_2 and τ_3 are chosen as

$$\tau_2 = (-\alpha_2 \dot{\theta}_2 + \beta_2 \Delta \theta_2 - \beta_1 \frac{A_{12}}{A_{11}} \Delta \theta_1), \tau_3 = (-\alpha_3 \dot{\theta}_3 + \beta_3 \Delta \theta_3 - \beta_1 \frac{A_{13}}{A_{11}} \Delta \theta_1) \quad (3.10)$$

where α_2 and α_3 are some arbitrary constants.

It is important to make one comment at this point. Equations (3.8) and (3.10) can both be used to plan the motion of the system. Equation (3.8) plans the motion at a kinematic level and Eq.(3.10) plans the motion at the dynamic level. While Eq.(3.10) is more complete in a sense, it neglects the presence of friction at the actuated joints. On the other hand, Eq.(3.8) can be used to provide the actuators with a reference trajectory. The actuators can then accurately track these trajectories using a PID control scheme. Then friction can be simply considered as external disturbances to the system.

C. PARAMETRIC UNCERTAINTIES AND UNMODELLED DYNAMICS

In this section we take into consideration the fact that the unactuated joint will have stiction and the damping parameter C of the rotary dashpot will not be a constant. The unactuated joint will use roller bearings and therefore we assume that the magnitude of stiction, which is unknown, is quite low. Furthermore, we assume that the nominal value of

the damping parameter is C and the true damping in the system is of the form

$$C(t) = \tilde{C} + \epsilon(t) \quad (3.11)$$

where we have assumed the damping in the system to be an implicit function of time. In reality the damping parameter will be an explicit function of the unactuated joint position, the temperature of the silicone fluid in the dashpot, etc.

We begin by stating that the generalized momentum corresponding to the first joint of the system is defined as

$$p_1 \triangleq (\partial L / \partial \dot{\theta}_1) = A_{11} \dot{\theta}_1 + A_{12} \dot{\theta}_2 + A_{13} \dot{\theta}_3 \quad (3.12)$$

and is a constant of the motion in the absence of external generalized forces. In our case there is stiction and viscous damping in the system that requires us to modify Eq.(3.1) of the form

$$\frac{dp_1}{dt} = -C(t) \dot{\theta}_1 - f_s \operatorname{sgn}(\dot{\theta}_1) \quad (3.13)$$

where f_s is the magnitude of the stiction that opposes torque and need not be assumed constant. From the above equation, we can write

$$dp_1 = -C(t) d\theta_1 - f_s \operatorname{sgn}(\dot{\theta}_1) dt \quad (3.14)$$

where the left hand side of Eq.(3.14) represents a change in the generalized momentum p_1 , and the right hand side represents the impulse of the non-conservative friction forces. We note here that dp_1 can be easily computed from the measured values of p_1 in successive sampling intervals. The expression for p_1 is given in Eq.(3.12) and can be computed at any instant from the measured values of the joint angles of the actuated joints and all the joint velocities.

We return to Eq.(3.13) and rewrite the system dynamics as

$$\frac{d}{dt} (A_{11}\dot{\theta}_1 + A_{12}\dot{\theta}_2 + A_{13}\dot{\theta}_3) + \tilde{C}\dot{\theta}_1 = -\epsilon(t)\dot{\theta}_1 - f_s \text{sgn}(\dot{\theta}_1) \quad (3.15)$$

which can be simplified to

$$(A_{11}\dot{\theta}_1 + A_{12}\dot{\theta}_2 + A_{13}\dot{\theta}_3 + \tilde{C}\dot{\theta}_1)_t - (A_{11}\dot{\theta}_1 + A_{12}\dot{\theta}_2 + A_{13}\dot{\theta}_3 + \tilde{C}\dot{\theta}_1)_{t_0} = \int_0^t \tilde{C}d\dot{\theta}_1 + dp_1 \quad (3.16)$$

by adopting the same method as in the last section, we provide the second joint with a "surge" velocity at the initial point of time such that Eq.(3.4) is satisfied while the first and the third joint are held fixed. Then we obtain from Eq.(3.16)

$$A_{11}\dot{\theta}_1 + A_{12}\dot{\theta}_2 + A_{13}\dot{\theta}_3 - \tilde{C}\Delta\dot{\theta}_1 = \int_0^t \tilde{C}d\dot{\theta}_1 + dp_1 \quad (3.17)$$

We redefine the Lyapunov function V_2 in Eq.(3.9) as V_3 , where we now treat θ_{2d} as a variable. We allow θ_{2d} to vary in

order to cancel the effect of any uncertainties and unmodelled dynamics that are present in the system. The derivative of the Lyapunov function is computed as

$$\begin{aligned} \dot{V}_3 = & \theta_2 (\tau_2 - \beta_2 \Delta \theta_2 + \beta_1 \frac{A_{12}}{A_{11}} \Delta \theta_1) + \theta_3 (\tau_3 - \beta_3 \Delta \theta_3 + \beta_1 \frac{A_{13}}{A_{11}} \Delta \theta_1) \\ & - \tilde{c} \theta_1^2 - \beta_1 \frac{\tilde{c}}{A_{11}} + [\beta_2 \Delta \theta_2 \theta_2 d - (\beta_1 \Delta \theta_1 / A_{11}) \int_0^t (\tilde{c} \alpha \theta_1 + d p_1)] \end{aligned} \quad (3.18)$$

Our choice of the control torques τ_2 and τ_3 as in Eq.(3.10) along with the choice of θ_{2d} as

$$\theta_{2d} = (\beta_1 \Delta \theta_1 / \beta_2 \Delta \theta_2 A_{11}) \int_0^t (\tilde{c} \alpha \theta_1 + d p_1) \quad (3.19)$$

results in the derivative of V_3 in Eq.(3.18) as negative definite and leads to the convergence of the unactuated joint and third joint to their desired values. Additionally, the second joint is converged to its desired configuration which is different from the initially specified value. The desired configuration of the second joint was not a constant but was made to follow a trajectory to compensate for the unmodelled friction forces. If the magnitude of the unmodelled stiction force and the uncertainty in the damping factor are small, the second joint will be converged to a value θ_{2d} at $(t=t_f)$ which will be quite close to the initial desired value of θ_2 , i.e. θ_{2d} at $(t=0)$. Therefore after the convergence of the Lyapunov function, the brake can be applied at the first joint and the

third joint can be held fixed at its desired configuration while the second joint is takes from its configuration θ_{2d} at $(t=t_f)$ to θ_{2d} at $(t=0)$.

IV RESULTS AND DISCUSSION

A. CONTROLLING OF JOINTS IN THE ABSENCE OF UNCERTAINTIES

We assume the three-link planar under-actuated manipulator, as shown in Fig.1, to have the following kinematic and dynamic parameters in S.I. units

Kinematic and Dynamic parameters			
	Mass	Inertia	Length
link-1	2.06	0.042917	$l_1=0.5$
link-2	2.06	0.042917	$l_2=0.5$
link-3	2.06	0.042917	$l_3=0.5$

All three links of the manipulator were assume to have a uniform mass distribution. In the first simulation, the initial and desired configuration of the system were assumed to be

$$(\theta_1, \theta_2, \theta_3) = (0.0, 45.0, 0.0)$$

$$(\theta_1, \theta_2, \theta_3) = (20.0, 0.0, 45.0)$$

(4.1)

and in the second simulation, the initial and the desired configurations were assumed to be

$$(\theta_1, \theta_2, \theta_3) = (10.0, 45.0, 5.0)$$

$$(\theta_1, \theta_2, \theta_3) = (22.5, 15.0, -25.0)$$

(4.2)

where the units were in degrees.

In both cases the damping constant was assumed to be 0.2 S.I. units and the criterion for the convergence of the lyapunov function was set at 5.0×10^{-5} . The evolution of the joint variables for the two simulations are shown in Figs.(2) and Fig.(3) respectively. In the first simulation convergence is achieved in only 11.5 seconds whereas the time taken for the second simulation is 12.0 seconds. In both cases, we see that the transition from initial position to final position is a smooth evolution. This is due to the absence of uncertainties in the system. We also notice that link 2 provides a surge velocity prior to the release of links 1 and 3. This surge velocity provides link 1 with the initial momentum needed to proceed in the proper direction for convergence. The surge velocity coupled with the motion of link two provides the control needed to bring link 1 to its final destination.

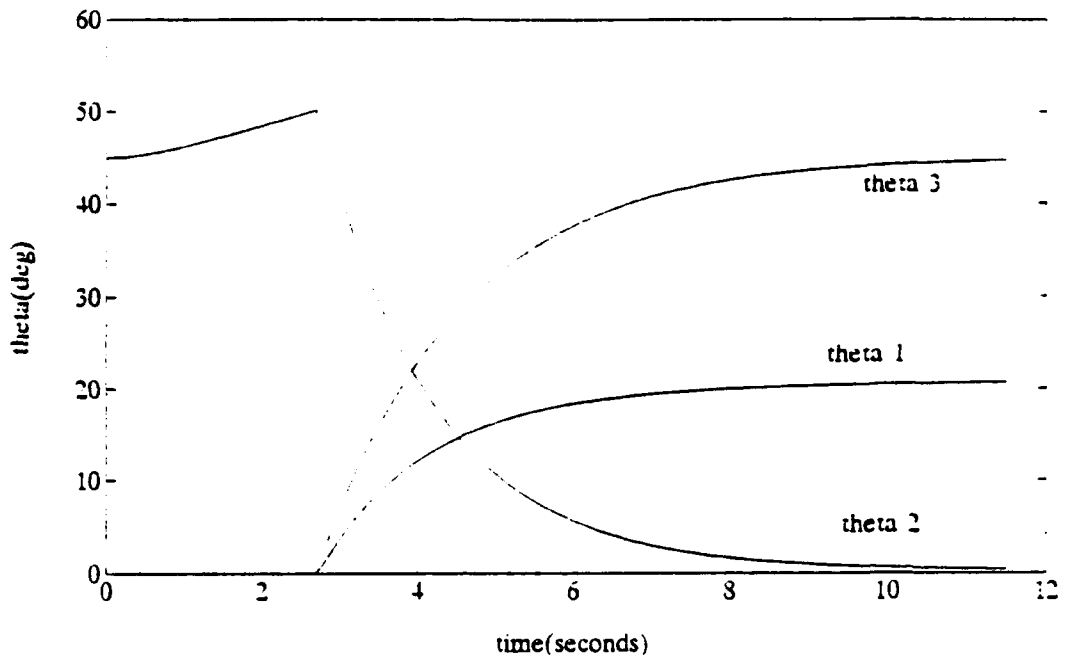


Figure 2: Evolution of joints for case one

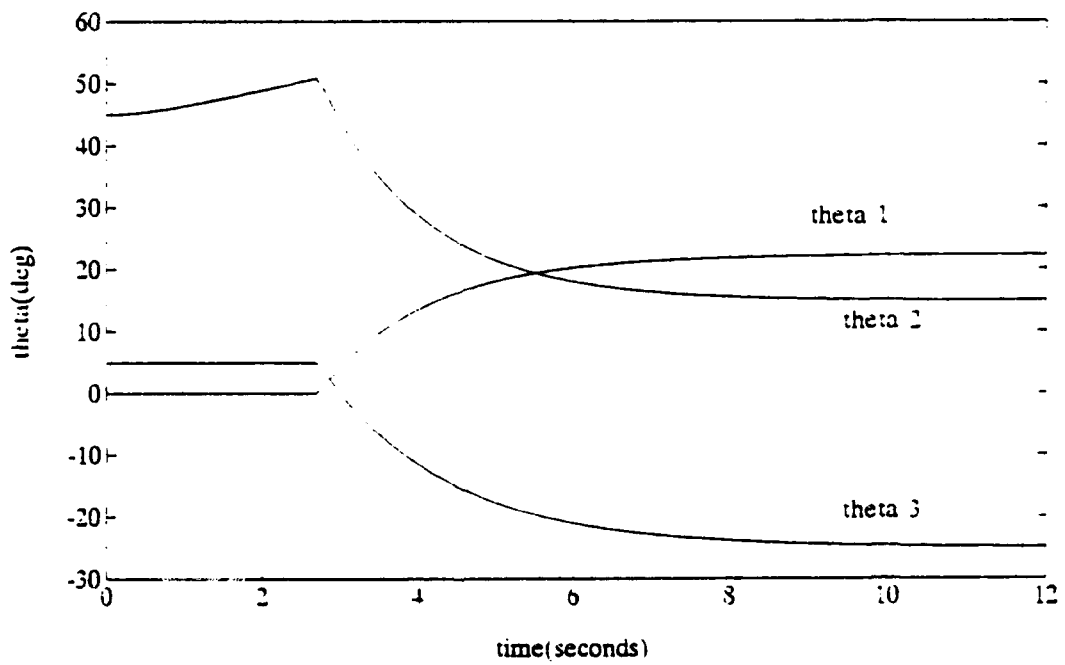


Figure 3: Evolution of joints for case two

B. CONTROLLING OF JOINTS WITH UNCERTAINTIES

The simulations are for the case in which parametric uncertainties and unmodelled dynamics exist. In this section, we shorten links 2 and 3 in order to further test the system. Smaller links will now be expected to control a larger link in addition to overcoming uncertainties that may be in the system. We assume the three link planar under-actuated manipulator to have the following kinematic and dynamic parameter in S.I. units.

Kinematic and Dynamic parameters			
	Mass	Inertia	length
link-1	2.06	0.043878	$l_1=0.5$
link-2	1.86	0.031881	$l_2=0.45$
link-3	1.65	0.022495	$l_3=0.4$

1. Variation of damping without stiction

As a next step, we simulate the case given by Eq. (4.1) but included timewise variation of damping at the unactuated joint. The variation of damping of the form

$$\epsilon(t) = .02\sin t + .015\cos t - .025\sin 4t$$

(4.3)

was imposed on the system. This is a slowly varying wave which varies within 25% of the nominal value, 0.2. We also

simulated the system for the case given by Eq.(4.1) with a damping whose variation is more abrupt at the unactuated joint. This variation of damping is of the form

$$\epsilon(t) = 0.1\bar{C}(\sin 5t + 0.33\sin 15t) \quad (4.4)$$

The two terms on the right hand side of Eq.(4.4) are the first two terms of the fourier expansion of a square wave with a time period of 0.2 seconds and an amplitude equal to 10% of the magnitude of the nominal value of damping. The variation of damping of Eq.(4.3) and Eq.(4.4) is shown in Fig.(4a) and Fig.(4b).

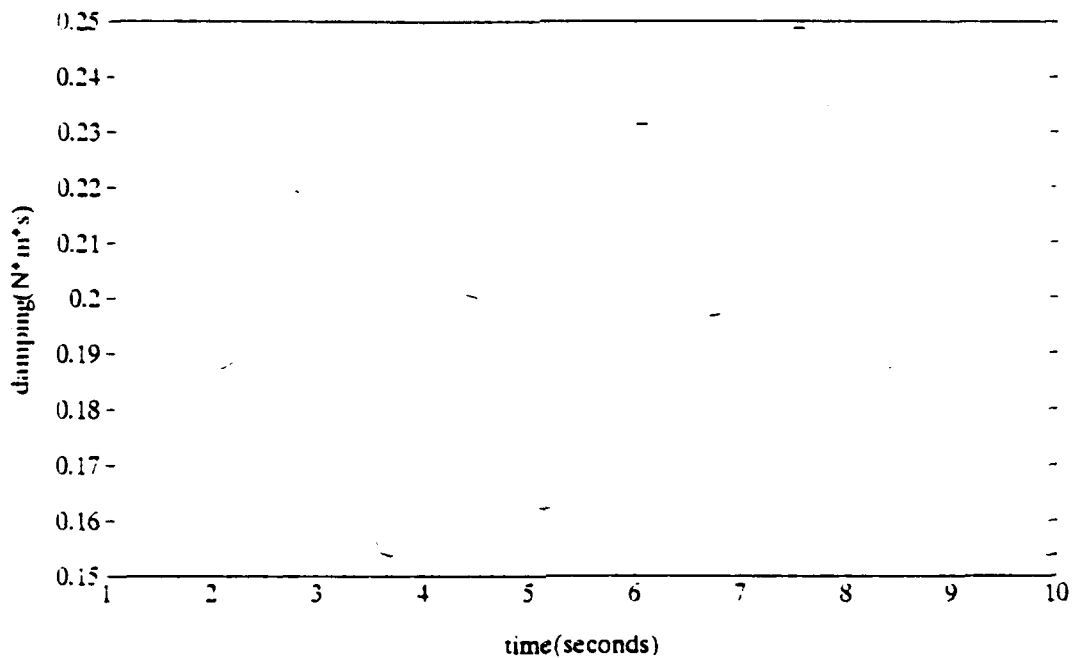


Figure 4a: Damping of the form described by Eq.(4.3)

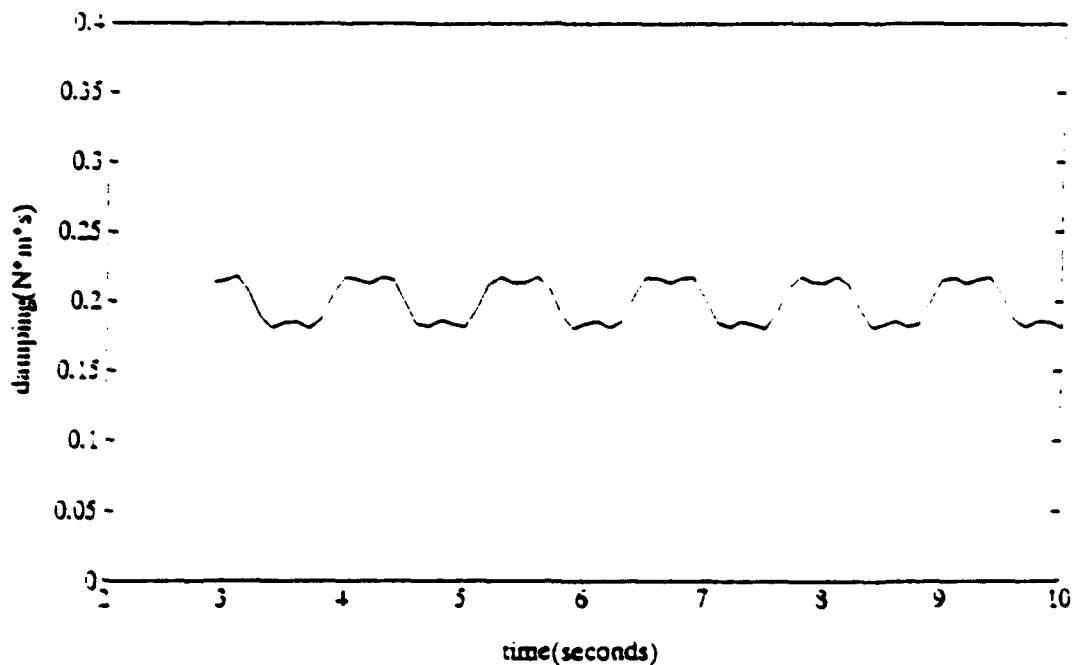


Figure 4b: Damping of the form described by Eq.(4.4)

The trajectory of the joint variables and θ_{2d} under the damping influence given by Eq.(4.3) is shown in Figs.(5a-5b). The time required for the simulation was only 8.3 seconds. All joints converged to its desired positions. The transitions of the links to their final positions were relatively smooth. The trajectories of the joint variables and θ_{2d} under the damping influence described by Eq.(4.4) are plotted in Figs.(6a-6b). The time required for the simulation was 11.3 seconds. The trajectory of the links are rather smooth. A shift from a negative slope to a positive slope is experienced by θ_{2d} . This shift is needed in order to bring link 1 to its final position. After θ_1 and θ_3 converge, a brake is applied and θ_2 is allowed to exponentially converge to its initial desired position.

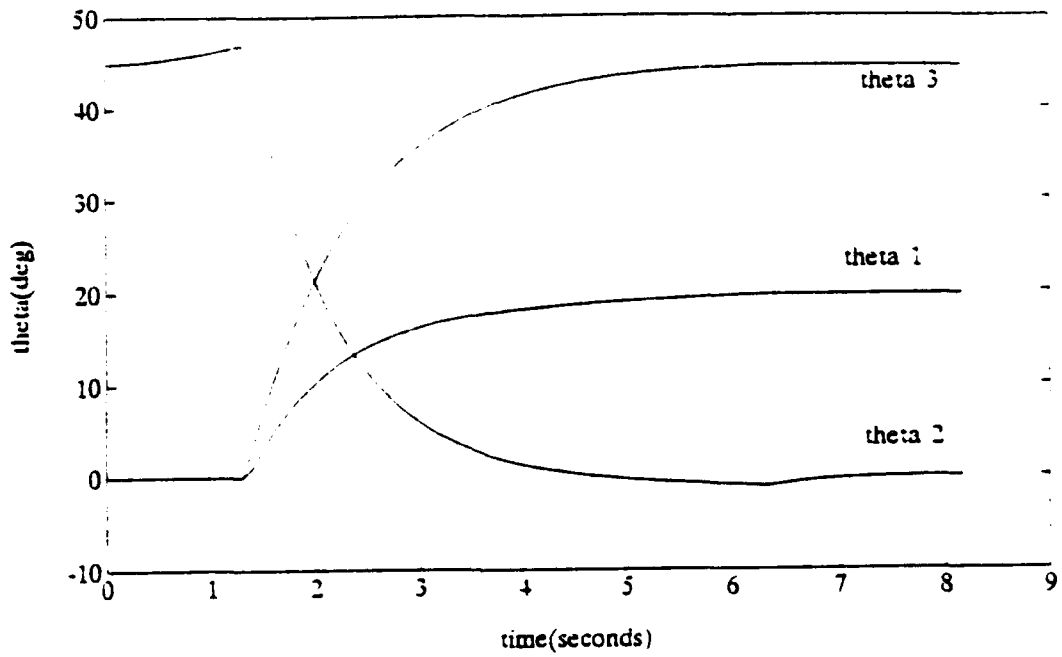


Figure 5a: Evolution of joints for case one under influence of damping given by Eq.(4.3)

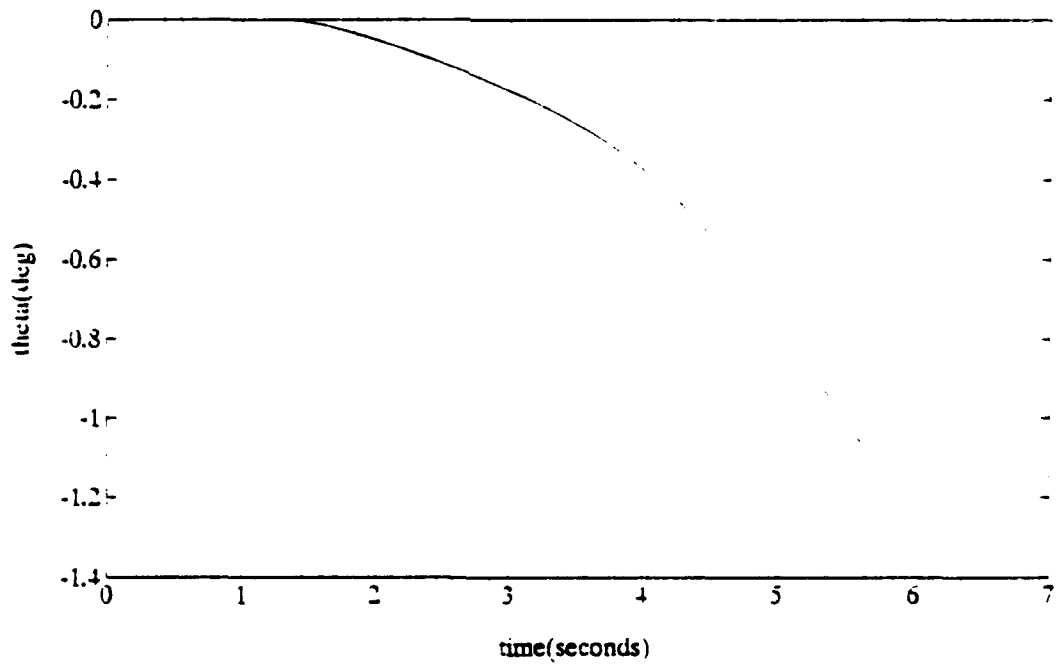


Figure 5b: Evolution of θ_{2d} for case one under influence of damping given by Eq.(4.3)

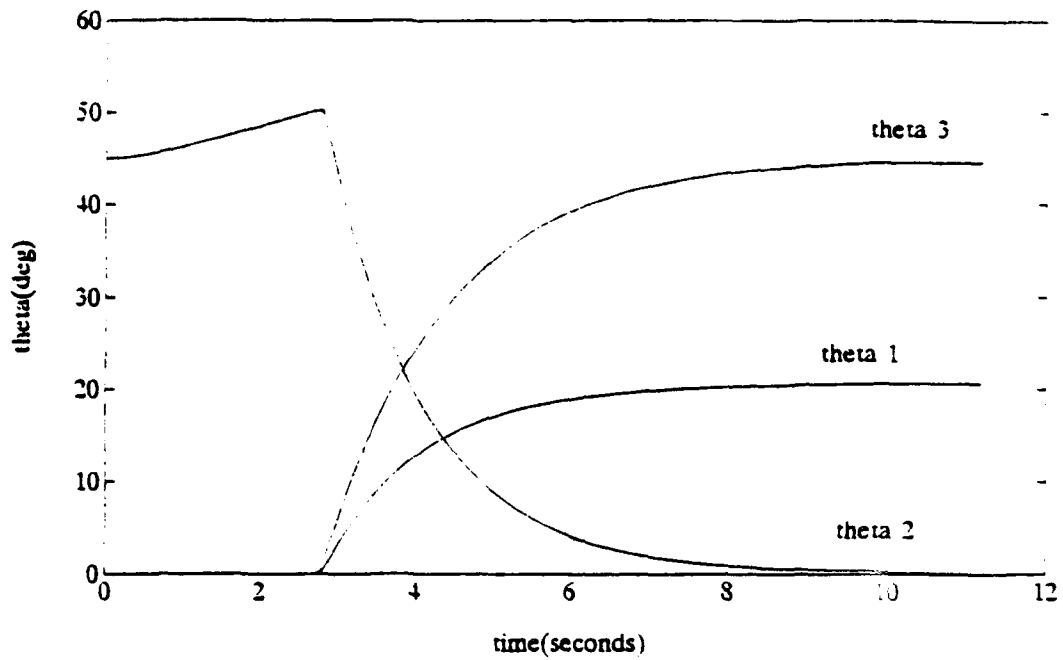


Figure 6a: Evolution of joints for case one under influence of damping given by Eq.(4.4)

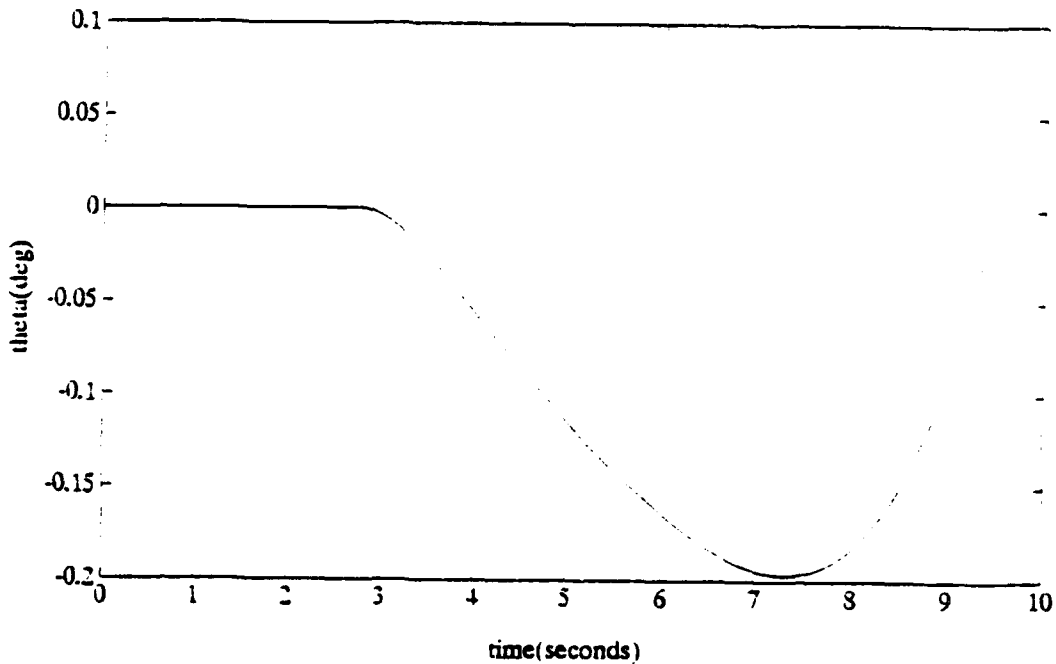


Figure 6b: Evolution of θ_{2d} for case one under influence of damping given by Eq.(4.4)

2. Variation of damping with stiction

a. Variation of damping given by Eq.(4.3)

As a next step, we simulate the same two cases given by Eq.(4.1) and Eq.(4.2) with the timewise variation in the coefficient of damping given by Eq.(4.3). We also include a stiction value of 0.001 Newton-meters. The trajectory of the joint variables and θ_{2d} is given in Figs.(7a-7b) for the case given by Eq.(4.1). The time for convergence was 15.2 seconds. The transition from the initial to final positions were smooth and uneventful, however, abrupt shifts was needed by θ_{2d} towards the end of the simulation in order for link 1 to converge. The trajectories for the second case are given in Figs.(8a-8b). The time for convergence was 24.5 seconds. It is evident that the trajectory given by Eq.(4.2) is more difficult to achieve than the one given by Eq.(4.1). There is more interaction between link 2 and link 1. It appears that θ_{2d} went to 15 degrees but after time it became evident that in order for link 1 to converge to its desired position θ_2 must decline. Sudden shifts of link 2 was needed to control link 1. Link 2 went below 10 degrees before it finally was allowed to exponentially converge at its desired position.

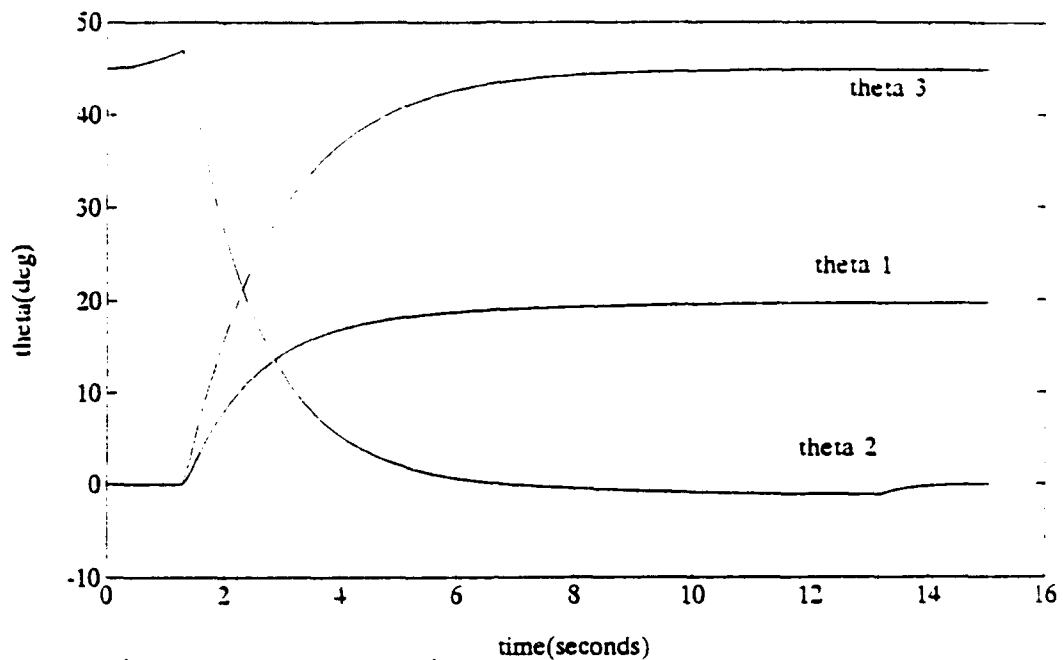


Figure 7a: Evolution of joints for case one under influence of damping given by Eq. (4.3) and a stiction value of 0.001.

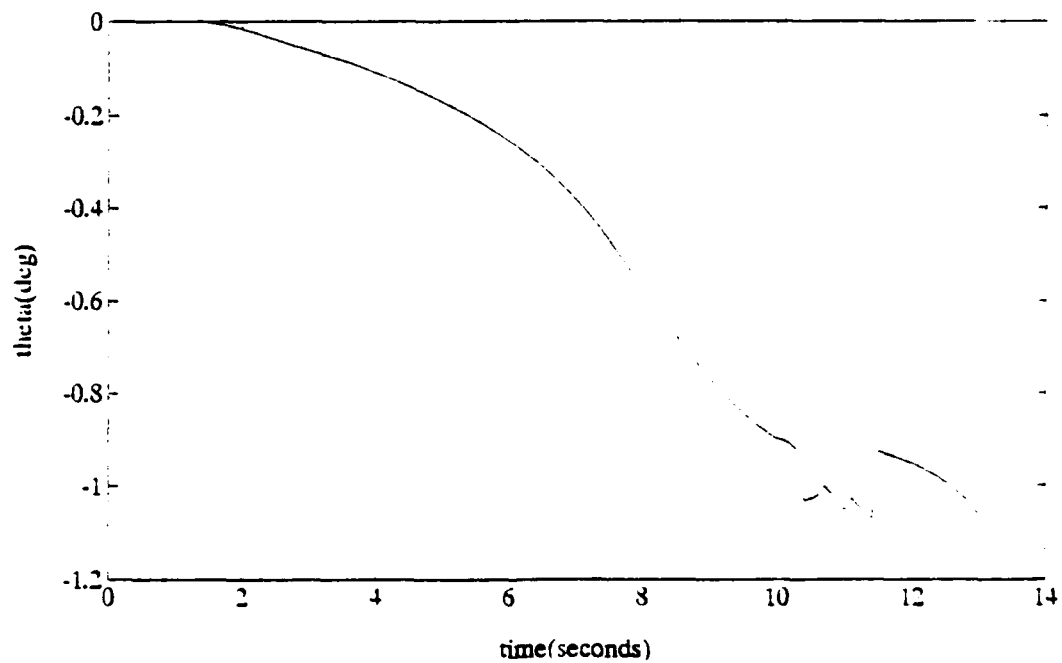


Figure 7b: Evolution of θ_{2d} for case one under influence of damping given by Eq. (4.3) and a stiction value of 0.001

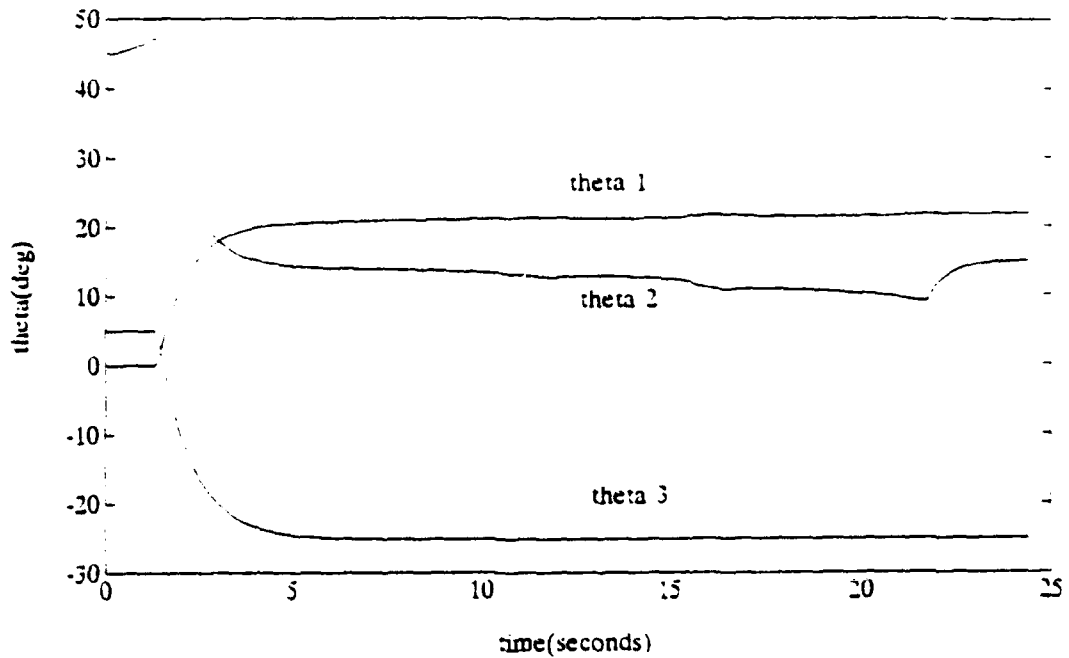


Figure 8a: Evolution of joints for case two under influence of damping given by Eq.(4.3) and a stiction value of 0.001

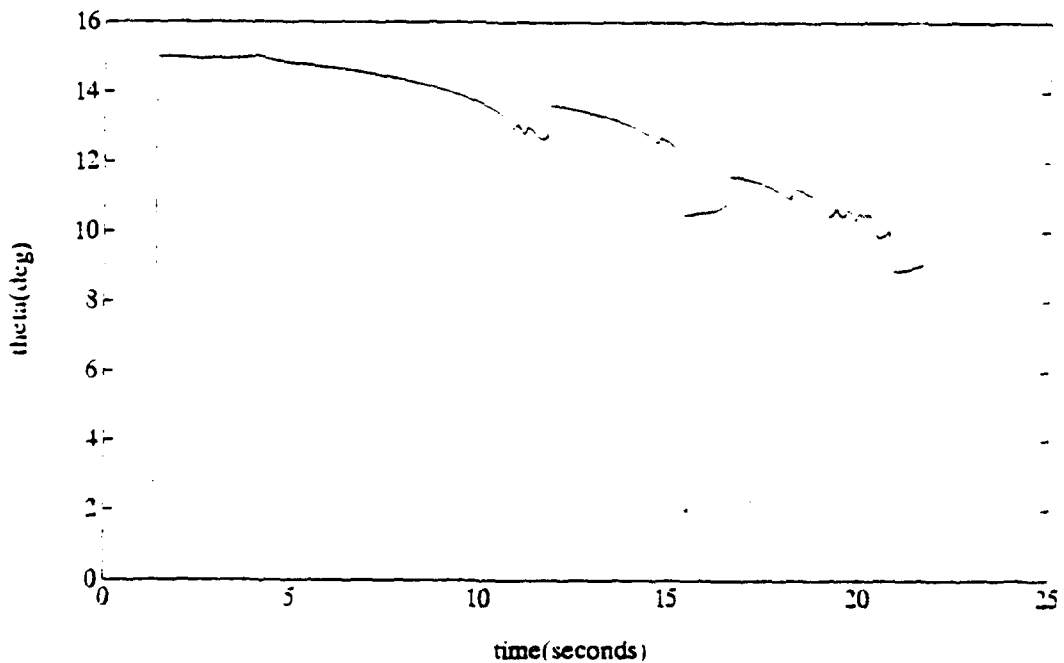


Figure 8b: Evolution of θ_{2d} for case two under influence of damping given by Eq.(4.3) and a stiction value of 0.001

b. Variation of damping given by Eq.(4.4)

In this section we simulate the same two cases given by Eqs.(4.1) and (4.2). The ratio of length of actuated links to the unactuated link was increased in order for the actuated links to have an increased influence. The timewise variation of damping given by Eq.(4.4) and an increased stiction value of 0.005 is applied to the unactuated joint. For the first case link 1 is decreased to 0.3 while link 2 and link 3 are increased to 0.8. The trajectories are given in Figs.(9a-9b). The time for convergence was 35.3 seconds. Small variations of link 2 at the end of the simulation was needed to bring link 1 to its desired position. A satisfactory simulation, however, the time for convergence was excessive. For the second case link 2 and link 3 was decreased to 0.6. The trajectories are given in Figs.(10a-10b). The time for convergence was 42.8 seconds. In both cases we find that the trajectory is not as abrupt as the results from the previous section, even though, the damping is more abrupt and the stiction is increased by a factor of five. This is due to the increase in length of the actuated links which gives them more control of the unactuated link. An attempt to simulate Eqs(4.1) and (4.2) under the damping given by Eq.(4.4) without changing the lengths of the links provided unsatisfactory results.

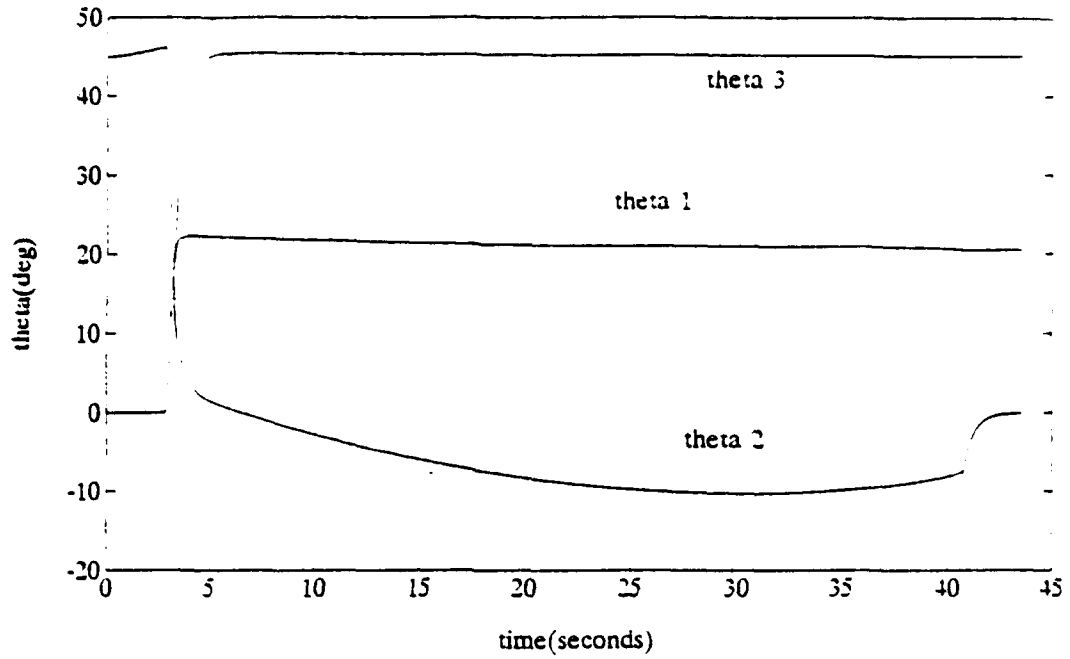


Figure 9a: Evolution of joints for case one under influence of damping given by Eq.(4.4) and a stiction value of 0.005

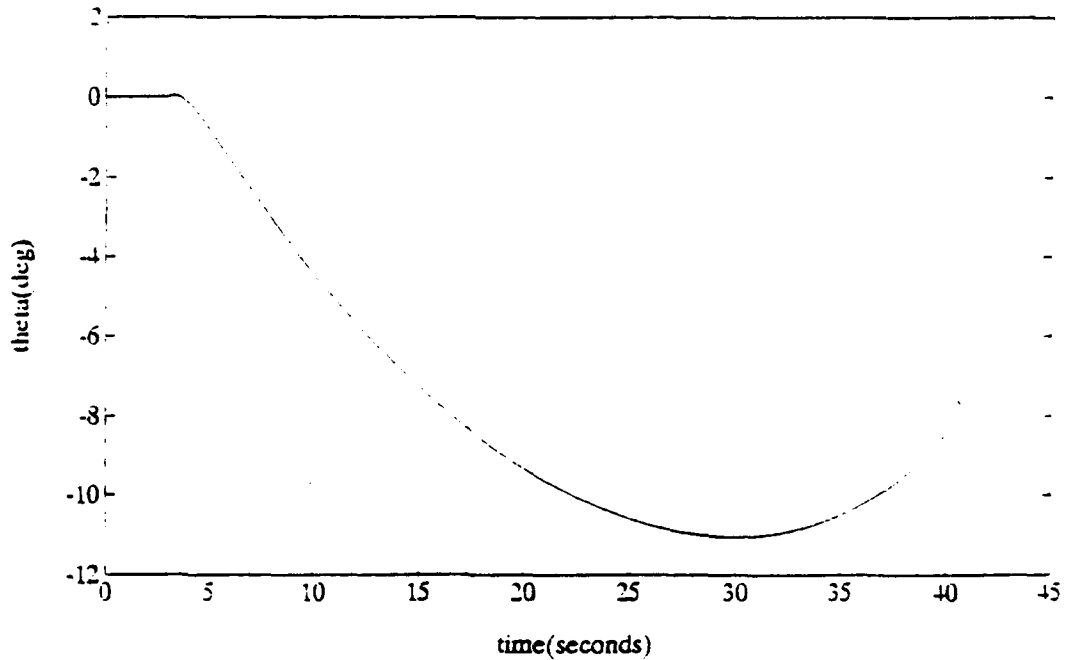


Figure 9b: Evolution of θ_{2d} for case one under influence of damping given by Eq.(4.4) and a stiction value of 0.005

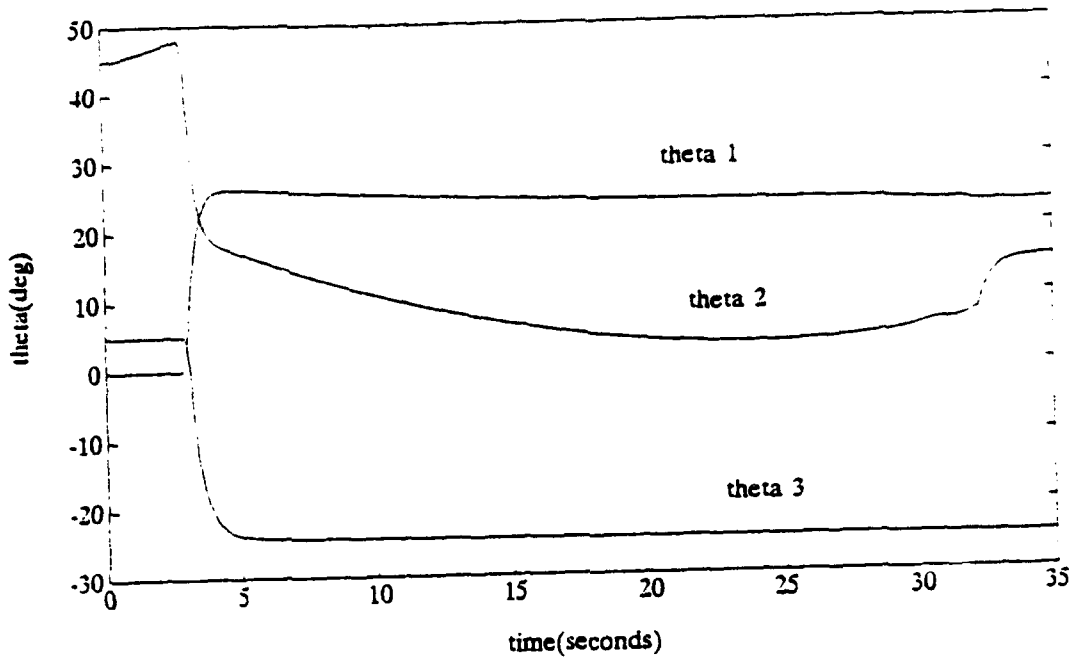


Figure 10a: Evolution of joints for case two under influence of damping given by Eq.(4.4) and a stiction value of 0.005

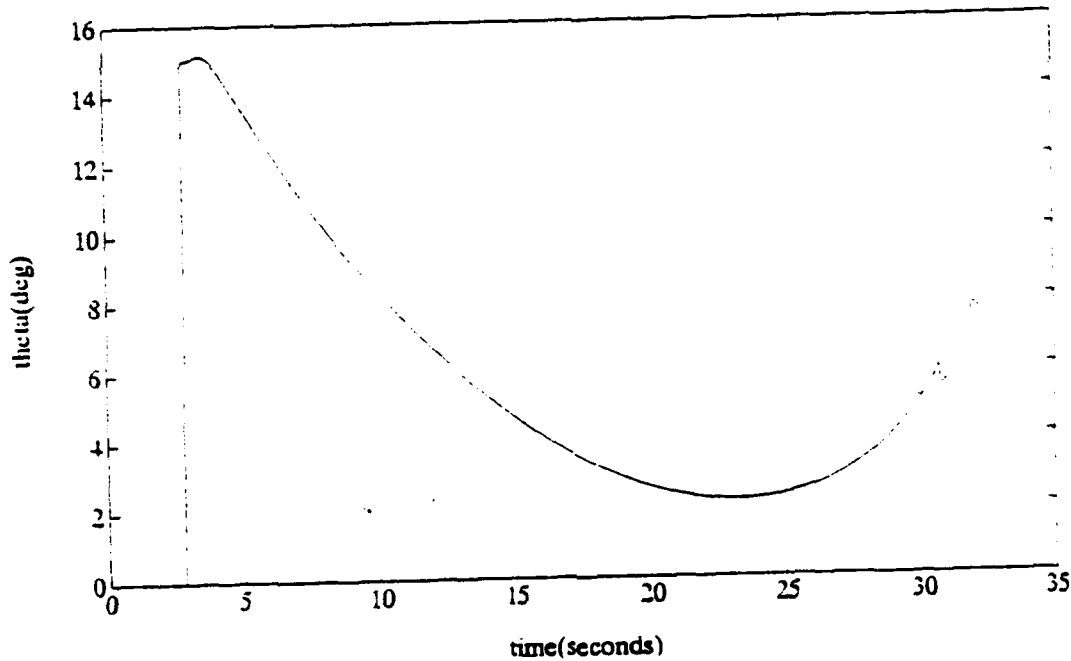


Figure 10b: Evolution of θ_{2d} for case two under influence of damping given by Eq.(4.4) and a stiction value of 0.005

V CONCLUSIONS AND RECOMMENDATIONS

Here we summarize our findings and we recommend future research directions as follows:

- From the simulation results it is quite clear that even in the presence of unmodelled dynamics and parametric uncertainties, it is possible to converge all the joints of the manipulator from their initial configuration to their desired configuration.
- It is apparent that the value of stiction can impair the ability of link 1 to converge to its desired value.
- It is obvious that increasing the ratio of length of the actuated links to link 1 will offset the stiction that is experienced by link 1.
- It is recommended that research be done with the increase in the mass ratio of the actuated links to link 1.
- It is recommended that a prototype of a three-link planar under-actuated manipulator be constructed so that a more accurate model can be simulated.
- It is recommended that further research be conducted with joint 2 or joint 3 unactuated and compared the model examined in this paper.
- In some of the simulations, θ_1 overshoot its intended target prior to settling on θ_{1d} . It is recommended that a simulation be performed that will stop link 1 instead of

allowing it to pass its target. A comparison of this model with the results presented in this paper should be performed.

LIST OF REFERENCES

- [1] Arai, H., and Tachi, S., 1991, "Position control of a manipulator with passive joints using dynamic coupling", IEEE Transactions on Robotics and Automation, Vol. 7, No. 4, pp. 528-534.
- [2] Jain, A., and Rodriguez, G., 1991, "Kinematics and Dynamics of Under-Actuated Manipulators", Proc. IEEE international Conference on Robotics and Automation, Vol. 2, pp 1754-1759.
- [3] Mukherjee, R., and Chen D., 1993, "Control of free-flying under-actuated space manipulators to equilibrium manifolds", Transactions of the IEEE on Robotics and Automation. (to appear).
- [4] Oriolo, G., and Nakamura, Y., 1991, "Nonholonomic motion of under-actuated kinematic chains", Proc. 9th Annual Conference of Japan Robotics Society, Tsukuba, Japan.

INITIAL DISTRIBUTION LIST

	No. Copies
1. Defense Technical Information Center Cameron Station Alexandria VA 22304-6145	2
2. Library, Code 052 Naval Postgraduate School Monterey CA 93943-5002	2
3. Professor Ranjan Mukherjee, CodeME/Mk Department of Mechanical Engineering Naval Postgraduate School Monterey CA 93943-5000	2
4. LT Pernell A. Jordan 1529 West First Street Dayton OH 45407	2